Published in "The Journal of Chemical Physics 123: 044106, 2005" which should be cited to reference this work

Higher-order response in $\mathcal{O}(N)$ by perturbed projection

Valéry Weber[a)]
Department of Chemistry, University of Fribourg, 1700 Fribourg, Switzerland

Anders M. N. Niklasson and Matt Challacombe[b)]
Los Alamos National Laboratory, Theoretical Division, Los Alamos 87545, New Mexico

(Received 21 December 2004; accepted 9 May 2005; published online 3 August 2005)

Perturbed projection for linear scaling solution of the coupled-perturbed self-consistent-field equations [V. Weber, A.M.N. Niklasson, and M. Challacombe, Phys. Rev. Lett. **92**, 193002 (2004)] is extended to the computation of higher-order static response properties. Although generally applicable, perturbed projection is further developed here in the context of the self-consistent first and second electric hyperpolarizabilities at the Hartree–Fock level of theory. Nonorthogonal, density-matrix analogs of Wigner's $2n+1$ rule valid for linear one-electron perturbations are given up to fourth order. Linear scaling and locality of the higher-order response densities under perturbation by a global electric field are demonstrated for three-dimensional water clusters.

I. INTRODUCTION

First-principles electronic structure theory has traditionally been limited to the study of small systems with a limited number of nonequivalent atoms. Despite the tremendous increase in computational power of digital computers this has remained the case, until the advent of reduced complexity algorithms over the last decade.[1–6] In the best case, these reduced complexity algorithms scale only linearly with the system size, N, allowing simulation capabilities to keep pace with hardware improvements. Linear scaling algorithms exploit the quantum locality (or nearsightedness) of nonmetallic systems, manifested in the approximate exponential decay of density-matrix elements with atom-atom separation through the effective use of sparse matrix methods. For small systems, linear scaling methods may be inefficient due to overhead. However, for large, complex systems these methods hold the promise of a major impact across materials science, chemistry, and biology.

So far, a majority of work in linear scaling electronic structure theory has focused on methods and calculations involving the ground state, with little attention devoted to the problem of response properties. The calculation of static response within Hartree–Fock or density-functional theory may be obtained through solution of the coupled-perturbed self-consistent-field (CPSCF) equations, which yield properties such as the electric polarizability and hyperpolarizability,[7,8] the Born-effective charge, the nuclear magnetic shielding tensor,[9] indirect spin-spin coupling constant,[10,11] geometric derivatives (i.e., higher-order analytic force constants),[12] and polarizability derivatives such as the Raman intensity,[13,14] to name but a few.

Conventional approaches to the solution of the CPSCF equations[7,8,15] are based on perturbation of the wave function, requiring an N^3-scaling eigensolve which may need to be followed by an $\mathcal{O}(N^5)$ transformation of two-electron integrals, depending on the method. In addition to the formal scaling of these conventional methods, they do not admit exploitation of quantum locality through the effective use of sparse matrix algebra. More recently, schemes with the potential for reduced complexity have been put forward. Ochsenfeld and Head-Gordon proposed a scheme based on the Li–Nunes–Vanderbilt density-matrix functional.[16] Later, Larsen *et al.*[17] proposed an iterative solution of the CPSCF equations involving equations derived from unitary operations and approximations to the matrix exponential. In both of these approaches, a linear system of equations containing commutation relations is obtained, which *implicitly* determines the response function. However, the method of solution for these equations is not discussed, and computational results are not presented. Recently though, with an apparent reformulation of the commutation relations presented in Ref. 16, Ochsenfeld *et al.*[18] claimed linear scaling computation of NMR chemical shifts for one-dimensional alcanes at the GIAO-HF/6-31G* level of theory, but likewise provided no details on their method of solution. Such commutation relations lead to equations of the Sylvester type and may be solved with a number of approaches,[19] the particulars of which are of interest.

In contrast, perturbed projection[20] is an alternative for N-scaling solution of the CPSCF equations that is simple and explicit. Based on a recently developed density-matrix perturbation theory,[21] perturbed projection exploits the direct relationship between the density matrix $\mathcal{D}$ and the effective Hamiltonian or Fockian $\mathcal{F}$ via spectral projection; $\mathcal{D}=\theta(\bar{\mu}I-\mathcal{F})$, wherein θ is the Heaviside step function (spectral projector) and the chemical potential $\bar{\mu}$ determines the occupied states via Aufbau filling. Spectral projection can be carried out in a number of ways.[22–29] Of special interest here are recursive polynomial expansions of the projector, including the second-order trace-correcting[22] (TC2) and fourth-order trace-resetting[23] (TRS4) purification algorithms. These new

[a)]Electronic mail: valery.weber@unifr.ch
[b)]Electronic mail: mchalla@lanl.gov

methods (TC2 and TRS4) have convergence properties that depend only weakly on the band gap, do not require knowledge of the chemical potential, and perform well for all occupation to state ratios. Perhaps most important to the current contribution, these methods converge rapidly to smooth, monotone projectors.

Perturbed projection has demonstrated linear scaling in computation of the first electric polarizability for three-dimensional water clusters with the Hartree–Fock model.[20] Also in a preceding paper, we outlined a nonorthogonal density-matrix perturbation theory[30] for response to a change in basis (e.g., as occurs in the evaluation of higher-order geometric energy derivatives[12]). In this article, the perturbed projection method is extended to higher orders in the electric polarizability, up to fourth order in the total energy.

This paper is organized as follows: First, we describe the perturbation expansion and the computation of response properties through solution of the CPSCF equations. Then we present extension of perturbed projection through higher orders and the computation of properties using a density-matrix analog of Wigner's $2n+1$ rule. Next, we present several examples of calculated higher-order response properties. We show the saturation of hyperpolarizabilities up to fourth order (i.e., up to the second hyperpolarizability γ) for a series of water chains. We also demonstrate linear scaling complexity for the solution of the higher-order CPSCF equations and an approximate exponential decay in elements of higher-order response functions for three-dimensional water clusters. Finally, we discuss these results and present our conclusions.

II. THE COUPLED-PERTURBED SELF-CONSISTENT-FIELD EQUATIONS

CPSCF equations yield static response functions and properties in models including both the Hartree–Fock (HF) and density-functional theory (DFT). In the following we develop perturbed projection for solution of the CPSCF equations in the framework of polarization and Hartree–Fock theory. In many cases, the extension of perturbed projection to the computation of other static perturbations is straightforward. In the case of model chemistries that involve DFT, an extra programming effort is required.[31,32] Also, in the case of properties such as the NMR chemical shift and geometric derivatives (force constants), perturbation of the nonorthogonal basis requires additional considerations that we have detailed in a preceding paper.[30]

A. Notation

The superscripts and subscripts refer to perturbation order and self-consistent cycle count, respectively. The symbols $\mathcal{D}, \mathcal{F}, \ldots$, are matrices in an orthogonal representation, while $D, F, \ldots$, are the corresponding matrices in a nonorthogonal basis. The transformation between orthogonal and nonorthogonal representations is carried out in $\mathcal{O}(N)$ using congruence transformations[33,34] provided by the approximate inverse (AINV) algorithm for computing sparse approximate inverse Cholesky factors with a computational complexity scaling linearly with the system size.[35–37]

B. Response expansions

Within HF theory, the total electronic energy E_{tot} of a molecule in a static electric field $\mathcal{E}$ is

$$E_{\mathrm{tot}}(\mathcal{E}) = \mathrm{Tr}\{D\cdot(h^0+\mu\mathcal{E})\} + \frac{1}{2}\mathrm{Tr}\{D\cdot(J[D]+K[D])\}$$
$$= \mathrm{Tr}\{D\cdot F[D]\} - \frac{1}{2}\mathrm{Tr}\{D\cdot(J[D]+K[D])\}, \quad (1)$$

where $D\equiv D[\mathcal{E}]$ is the density matrix in the electric field $\mathcal{E}$, h^0 is the core Hamiltonian, μ is the dipole moment matrix, $J[D]$ is the Coulomb matrix, $K[D]$ the exact HF exchange matrix, and

$$F \equiv F[\mathcal{E}] = h^0 + \mu\mathcal{E} + J[D(\mathcal{E})] + K[D(\mathcal{E})] \quad (2)$$

is the Fockian. The total energy of a molecule in a homogeneous electric field may be developed in a Taylor-series expansion around $\mathcal{E}=0$ as

$$E_{\mathrm{tot}}(\mathcal{E}) = E_{\mathrm{tot}}(0) - \sum_a \mu_a\mathcal{E}^a - \frac{1}{2!}\sum_{ab}\alpha_{ab}\mathcal{E}^a\mathcal{E}^b$$
$$- \frac{1}{3!}\sum_{abc}\beta_{abc}\mathcal{E}^a\mathcal{E}^b\mathcal{E}^c - \frac{1}{4!}\sum_{abcd}\gamma_{abcd}\mathcal{E}^a\mathcal{E}^b\mathcal{E}^c\mathcal{E}^d + \ldots, \quad (3)$$

where α_{ab} is the polarizability, β_{abc} and γ_{abcd} are the first and second hyperpolarizabilities, respectively, μ_a is the dipole moment, and $\mathcal{E}^a$ is the electric field in direction a. The polarizability α_{ab} is the second-order response of the total energy with respect to variation in the electric field while the higher derivatives, β_{abc} and γ_{abcd}, give rise to the first and second hyperpolarizabilities,[7,8] where

$$\alpha_{ab} = -\left.\frac{\partial^2 E_{\mathrm{tot}}}{\partial\mathcal{E}^a\,\partial\mathcal{E}^b}\right|_{\mathcal{E}=0} = -2\,\mathrm{Tr}[D^a\mu_b], \quad (4a)$$

$$\beta_{abc} = -\left.\frac{\partial^3 E_{\mathrm{tot}}}{\partial\mathcal{E}^a\,\partial\mathcal{E}^b\,\partial\mathcal{E}^c}\right|_{\mathcal{E}=0} = -2\,\mathrm{Tr}[D^{ab}\mu_c], \quad (4b)$$

$$\gamma_{abcd} = -\left.\frac{\partial^4 E_{\mathrm{tot}}}{\partial\mathcal{E}^a\,\partial\mathcal{E}^b\,\partial\mathcal{E}^c\,\partial\mathcal{E}^d}\right|_{\mathcal{E}=0} = -2\,\mathrm{Tr}[D^{abc}\mu_d]. \quad (4c)$$

Here $D^{a\cdots}$ denotes a density-matrix derivative with respect to a field in directions $a\ldots$ at $\mathcal{E}=0$ and the factor 2 accounts for the orbital occupation. The density-matrix derivative or "response function" is given by

$$\mathcal{D}^{a\cdots} = \left.\frac{\partial^n}{\partial\mathcal{E}^{a\ldots}}\theta(\tilde{\mu}I-\mathcal{F}(\mathcal{E}))\right|_{\mathcal{E}=0}. \quad (5)$$

The Fockian may also be expanded order by order in the perturbation to yield

$$\mathcal{F}(\mathcal{E}) = \mathcal{F}^0 + \sum_a \mathcal{F}^a\mathcal{E}^a + \frac{1}{2!}\sum_{ab}\mathcal{F}^{ab}\mathcal{E}^a\mathcal{E}^b$$
$$+ \frac{1}{3!}\sum_{abc}\mathcal{F}^{abc}\mathcal{E}^a\mathcal{E}^b\mathcal{E}^c + \ldots, \quad (6)$$

where $\mathcal{F}^a$ stands for $\partial\mathcal{F}(\mathcal{E})/\partial\mathcal{E}^a$, $\mathcal{F}^{ab}=\partial^2\mathcal{F}(\mathcal{E})/\partial\mathcal{E}^a\partial\mathcal{E}^b$, and

so on for the higher-order terms. A similar expansion also holds for the density matrix $\mathcal{D}(\mathcal{E})$.

Within HF theory, the unperturbed Fockian F^0 in the nonorthogonal basis is

$$F^0 = h^0 + J(D^0) + K(D^0), \tag{7}$$

while the first variation of the Fockian is

$$F^a = \mu_a + J(D^a) + K(D^a), \tag{8}$$

and the higher terms are given by

$$F^{ab\cdots} = J(D^{ab\cdots}) + K(D^{ab\cdots}). \tag{9}$$

In computation of the unperturbed Fockian, the Coulomb matrix J may be computed in $\mathcal{O}(N \lg N)$ with the quantum chemical tree code[38] (QCTC) and the exchange matrix K computed in $\mathcal{O}(N)$ with the $\mathcal{O}(N)$-exchange (ONX) algorithm that exploits quantum locality of the density matrix D^0.[39] Likewise the Fockian derivatives, $F^{a\cdots}$, may be computed with the same algorithms in linear scaling time if elements of $D^{a\cdots}$ manifest an approximate exponential decay with atom-atom separation, similar to the decay properties of D^0.

While the expansions above are given explicitly for Hartree–Fock theory, similar expressions hold also for Kohn–Sham and hybrid HF/DFT, which involve variation of the exchange-correlation matrix $V_{xc}^{a\cdots}(D^0, D^a, \ldots)$.[31,32]

C. Conditions for self-consistency

The derivative density matrices and derivative Fockians depend on each other implicitly, and must be solved self-consistency via the CPSCF equations. The necessary and sufficient criteria for convergence of the CPSCF equations involve generalized self-consistence conditions that were obtained from perturbative expansion of the SCF commutation criteria,[40]

$$[\mathcal{F}^0, \mathcal{D}^0] = 0, \tag{10}$$

$$[\mathcal{F}^a, \mathcal{D}^0] + [\mathcal{F}^0, \mathcal{D}^a] = 0, \tag{11}$$

$$[\mathcal{F}^{ab}, \mathcal{D}^0] + [\mathcal{F}^a, \mathcal{D}^b] + [\mathcal{F}^b, \mathcal{D}^a] + [\mathcal{F}^0, \mathcal{D}^{ab}] = 0, \tag{12}$$

$$[\mathcal{F}^{abc}, \mathcal{D}^0] + [\mathcal{F}^{ab}, \mathcal{D}^c] + [\mathcal{F}^{ac}, \mathcal{D}^b] + [\mathcal{F}^{ab}, \mathcal{D}^c] + [\mathcal{F}^a, \mathcal{D}^{bc}] + [\mathcal{F}^b, \mathcal{D}^{ac}] + [\mathcal{F}^c, \mathcal{D}^{ab}] + [\mathcal{F}^0, \mathcal{D}^{abc}] = 0, \tag{13}$$

in addition to the idempotency constraints,[40]

$$\mathcal{D}^0 = \mathcal{D}^0\mathcal{D}^0, \tag{14}$$

$$\mathcal{D}^a = \{\mathcal{D}^a, \mathcal{D}^0\}, \tag{15}$$

$$\mathcal{D}^{ab} = \{\mathcal{D}^{ab}, \mathcal{D}^0\} + \{\mathcal{D}^a, \mathcal{D}^b\}, \tag{16}$$

$$\mathcal{D}^{abc} = \{\mathcal{D}^{abc}, \mathcal{D}_0\} + \{\mathcal{D}^{ab}, \mathcal{D}^c\} + \{\mathcal{D}^{ac}, \mathcal{D}^b\} + \{\mathcal{D}^{bc}, \mathcal{D}^a\}, \tag{17}$$

where the anticommutator notation $\{A, B\} = AB + BA$ has been used.

III. SOLVING THE HIGHER-ORDER CPSCF EQUATIONS WITH PERTURBED PROJECTION

In the solution of the CPSCF equations, it is first necessary to determine the ground-state density matrix $\mathcal{D}^0$. This may be accomplished in $\mathcal{O}(N)$ using a purification algorithm such as Niklasson's[22] second-order trace-correcting scheme (TC2) in conjunction with sparse atom-blocked linear algebra.[23,41] Linear scaling is achieved for insulating systems through the dropping (filtering) of atom-atom blocks with Frobenious norm below a numerical threshold ($\tau \sim 10^{-4}$–10^{-7}). At SCF convergence the TC2 algorithm generates a polynomial sequence defining the ground-state projector, from which the derivative density matrices are obtained directly.

Having solved the ground-state SCF equations, solution of the CPSCF equations commences with a guess at the derivative densities (i.e., $D_0^{a\cdots} = 0$), followed by computation of derivative Fockians. At the rth CPSCF cycle, the nth-order derivative Fockians are

$$F_r^{a\cdots} = \begin{cases} \mu_a + J(D_r^a) + K(D_r^a), & n = 1 \\ J(D_r^{a\cdots}) + K(D_r^{a\cdots}), & n > 1. \end{cases} \tag{18}$$

After construction of the derivative Fockians, response functions through $D_{r+1}^{a\cdots}$ are computed, constituting one cycle in solution of the CPSCF. As described in Sec. III A, these response functions are obtained directly through variation of the occupied subspace projector,

$$D_{r+1}^{a\cdots} = \left. \frac{\partial^n}{\partial \mathcal{E}^{a\cdots}} \theta(\tilde{\mu} I - \mathcal{F}_r(\mathcal{E})) \right|_{\mathcal{E}=0}, \tag{19}$$

which is accomplished via perturbed projection, a subset of the Niklasson and Challacombe density-matrix perturbation theory[21] corresponding to the solution of the CPSCF equations. However, in contrast with Ref. 21, a Taylor-series expansion is employed here, consistent with previous work on the polarization tensor.

After a few CPSCF cycles, the approach to self-consistency may be accelerated with Weber and Daul's DDIIS algorithm,[42]

$$\tilde{\mathcal{F}}_r^{a\cdots} = \sum_{k=r-s}^{r} c_k \mathcal{F}_k^{a\cdots}, \tag{20}$$

in which the c_k coefficients are chosen to minimize the nth-order commutation relations, as in Eqs. (11)–(13). The application of the DDIIS algorithm to the acceleration of higher-order CPSCF equations is developed further in Sec. III B. At self-consistency, the conditions given in Sec. II C have been met, and it is then appropriate to compute response properties. In general, we can obtain an expectation value for properties that is linear in the response functions through direct, order by order expansion of Eq. (1). In the case of polarization, and other properties that involve a linear one-electron perturbation $h^{(1)}$, expressions for the total-energy response reduce to

$$E_{\text{tot}}^{(\gamma+1)} = 2\ \text{Tr}(D^{(\gamma)} h^{(1)}), \tag{21}$$

consistent with Eqs. (4a)–(4c) for the (hyper)polarizabilities.

A. Perturbed projection

Although a number of analytic, asymptotically discontinuous representations exist for the Heaviside step function θ, direct representation (and variation) of these forms as in Eq. (19) is problematic. Polynomial expansion of the step function is an alternative choice[43] but demands a very high order and can be costly. Specifically, polynomial expansion of θ with a p'th-order polynomial incurs a cost that is at best $\mathcal{O}(\sqrt{p})$.[44,45] Polynomial expansion techniques, such as those based on the the Chebychev polynomials, may also be plagued by Gibbs oscillations,[46] which are high-order ripples in the approximate θ due to incompleteness. Alternatively, recursive purification methods achieve high-order representation in $\mathcal{O}(\log p)$.[23] In addition, purification methods (such as TC2 and TRS4) yield projectors that are smooth and strictly monotonic.

Each perturbed projection sequence is based on a corresponding purification scheme or generator, such as TC2.[22] The perturbed projection sequence is obtained by collecting terms of the response order by order upon perturbative expansion of its generator.[21] Perturbed projection provides explicit, recursive formulas for the construction of response functions, retaining the convergence properties, smoothness, and monotonicity of the generating sequence. These explicit formulas-stand in contrast with methods where the density-matrix derivatives are implicitly defined as solutions to equations of Sylvester type.[16–18]

Sufficient to compute fourth-order properties using the $2n+1$ rule presented in Sec. III C, perturbed projection is outlined in the following for computation of the second-order response function: the perturbed projection sequence is started with the $\mathcal{X}_0^{a\cdots}$, which are prepared from the Fockian $\mathcal{F}^0$ and its derivatives $\mathcal{F}^a$ and $\mathcal{F}^{ab}$ by mapping their spectrum into the domain of convergence[22] using

$$\mathcal{X}_0^0 = \frac{\mathcal{F}_{\max} I - \mathcal{F}^0}{\mathcal{F}_{\max} - \mathcal{F}_{\min}} \tag{22}$$

and

$$\mathcal{X}_0^{a\cdots} = \frac{\mathcal{F}_n^{a\cdots}}{\mathcal{F}_{\min} - \mathcal{F}_{\max}}, \tag{23}$$

where $\mathcal{F}_{\min}$ and $\mathcal{F}_{\max}$ are the upper and lower bounds to the eigenvalues of $\mathcal{F}^0$.

While perturbed projection can be formulated within any purification scheme, we focus here on the simple and efficient TC2 method.[22] Briefly, TC2 constructs a ground-state projector through a series of trace-correcting projections; when the trace is larger than N_e, x^2 is used to reduce the trace, and when the trace is less than N_e, $2x-x^2$ is used to increase the trace. The resulting sequence of correcting projections yields a step at the correct chemical potential. Within this framework, the second-order TC2 perturbed projection sequence is

$$\left.\begin{aligned} \mathcal{X}_{i+1}^{ab} &= \{\mathcal{X}_i^{ab}, \mathcal{X}_i^0\} + \{\mathcal{X}_i^a, \mathcal{X}_i^b\} \\ \mathcal{X}_{i+1}^{a} &= \{\mathcal{X}_i^{a}, \mathcal{X}_i^0\} \\ \mathcal{X}_{i+1}^{b} &= \{\mathcal{X}_i^{b}, \mathcal{X}_i^0\} \\ \mathcal{X}_{i+1}^{0} &= (\mathcal{X}_i^0)^2 \end{aligned}\right\} \mathrm{Tr}[\mathcal{X}_i^0] \geqslant N_e \tag{24}$$

or

$$\left.\begin{aligned} \mathcal{X}_{i+1}^{ab} &= 2\mathcal{X}_i^{ab} - (\{\mathcal{X}_i^{ab}, \mathcal{X}_i^0\} + \{\mathcal{X}_i^a, \mathcal{X}_i^b\}) \\ \mathcal{X}_{i+1}^{b} &= 2\mathcal{X}_i^{b} - \{\mathcal{X}_i^{b}, \mathcal{X}_i^0\} \\ \mathcal{X}_{i+1}^{a} &= 2\mathcal{X}_i^{a} - \{\mathcal{X}_i^{a}, \mathcal{X}_i^0\} \\ \mathcal{X}_{i+1}^{0} &= 2\mathcal{X}_i^{0} - (\mathcal{X}_i^0)^2 \end{aligned}\right\} \mathrm{Tr}[\mathcal{X}_i^0] < N_e. \tag{25}$$

As with the TC2 generator, the nth-order response functions

$$\mathcal{D}^{a\cdots} = \lim_{i\to\infty} \mathcal{X}_i^{a\cdots}, \tag{26}$$

converges quadratically, reaching convergence when either the error $\varepsilon = |\mathrm{Tr}[\mathcal{X}_i^0] - N_e| + |\mathrm{Tr}[\mathcal{X}_i^a]| + \ldots$, or the maximum element in the change $\delta\mathcal{X}^{a\cdots} = |\mathcal{X}_{i+1}^{a\cdots} - \mathcal{X}_i^{a\cdots}|$ falls below τ, the atom-atom block drop tolerance described in Ref. 23. As outlined in Ref. 30, when the solution gets close to convergence, i.e., $|\mathrm{Tr}[\mathcal{X}_i^0] - N_e| < \epsilon$ with $\epsilon \approx 10^{-1} - 10^{-3}$, we alternate the projection at each step, which protects the convergence under the incomplete sparse linear algebra.

B. Derivative DIIS

Direct inversion in the iterative subspace (DIIS), introduced some time ago by Pulay,[47,48] accelerates convergence toward self-consistency. DIIS employs information accumulated during preceding iterations to construct an effective Fockian $\tilde{\mathcal{F}}_k$ at the kth SCF cycle, which minimizes the commutation error between the Fockian and the density matrix. The effective Fockian is then used instead of $\mathcal{F}_k$ to generate an improved density matrix.

Recently, Weber and Daul have developed the derivative DIIS (DDIIS) scheme for accelerating convergence of the CPSCF equations.[42] Like DIIS, DDIIS is based on minimization of the Frobenious norm of an error matrix

$$\tilde{e}_r^{a\cdots} = \sum_{i=r-s}^{r} c_i e_i^{a\cdots}, \tag{27}$$

where the $e_i^{a\cdots}$'s are just the nth-order commutator relation of Eqs. (10)–(13) (e.g., the first-order error matrix is given by $e_i^a = [\mathcal{F}_i^a, \mathcal{D}^0] + [\mathcal{F}^0, \mathcal{D}_i^a]$). The optimal coefficients c_i are solutions to the quadratic programming problem

$$\inf\left\{ -\frac{1}{2}\sum_{i,j=r-s}^{r} c_i B_{ij} c_j,\ \sum_{i=r-s}^{r} c_i = 1 \right\}, \tag{28}$$

where elements of the **B** matrix are given by $B_{ij} = \mathrm{Tr}[e_i^{a\cdots}(e_j^{a\cdots})^T]$. A working equation is then obtained through the associated Euler–Lagrange equation

$$\begin{pmatrix} \mathbf{B} & \mathbf{1} \\ \mathbf{1}^T & 0 \end{pmatrix} \cdot \begin{pmatrix} \mathbf{c} \\ \lambda \end{pmatrix} = \begin{pmatrix} \mathbf{0} \\ 1 \end{pmatrix}, \tag{29}$$

where $\mathbf{0}=(0,\ldots,0)^T$ and $\mathbf{1}=(1,\ldots,1)^T$ are vectors whose components are 0 and 1, respectively, and λ is the Lagrange multiplier of the constraint $\Sigma_{i=n-m}^{n} c_i=1$. The set of linear equations is solved by inverting the left-hand-side matrix. In the event of a singular or near singular matrix, the rank of Eq. (29) is reduced by discarding the oldest entries (increasing s) until the linear system stabilizes.

C. Density-matrix formulation of Wigner's 2n+1 rule

Wigner's $2n+1$ rule, traditionally predicated on derivatives of the wave function, yields order $2n+1$ in the energy response from nth-order derivatives.[8,49] A density-matrix analog of Wigner's $2n+1$ rule for a linear one-electron perturbation was given to third order by McWeeny[50] and up to to fourth order by Niklasson and Challacombe[21] in the orthogonal representation, suitable for first-order perturbation.

In the framework of electric polarizabilities, we present nonorthogonal $2n+1$ rules up to fourth order in response of the total energy. This new formulation includes mixed perturbations, accounts for self-consistency, and may be generalized to other linear one-electron perturbations. However, this formulation may not be extended to basis-set-dependent perturbations; that case is addressed by Ref. 30.

The first- and second-order energy corrections to electric perturbations are well known, corresponding simply to expectation values as in Eq. (21). Beyond second order, the $2n+1$ rule offers a valuable alternative to compute higher-order polarizabilites. The third-order nonorthogonal contribution is

$$\beta_{abc} = -2 \sum_{P(a,b,c)} \mathrm{Tr}[[D^a,D^0]_S S D^b F^c], \tag{30}$$

where $P(a,b,c)$ stands for the permutation operator such that all permutations of a, b, and c are made [e.g., $P(a,b,c)$ generates the sum of all the six terms: (a,b,c), (a,c,b), (b,a,c), (b,c,a), (c,a,b), and (c,b,a)] and $[A,B]_S=ASB-BSA$ where S is the overlap matrix. Similarly, the fourth-order nonorthogonal contribution is

$$\gamma_{abcd} = -\frac{1}{2} \sum_{P(a,b,c,d)} \mathrm{Tr}[[D^{ab},D^0]_S S D^c F^d + [D^a,D^0]_S S (D^{bc}F^d + D^b F^{cd})]. \tag{31}$$

For the orthogonal case $S=I$ and D^a, F^c, …, are replaced by $\mathcal{D}^a$, $\mathcal{F}^c$, …. In most cases the complexity of these equations can be reduced by taking advantage of indicial symmetry; a, b, c, and d represent the Cartesian directions x,y,z so that terms with indices in the same direction simplify. For example, γ_{aaaa} reduces to one term requiring only 15 matrix multiplications. In the worst case, where all the directions are different, i.e., γ_{aabc} [or any other permutation of (a,a,b,c)], the relation (31) reduces to include only 12 terms with 180 matrix multiplications. Similar reductions of the computational cost also apply to Eq. (30). The number of matrix-matrix multiplies can be further reduced if one uses an orthogonal representation, but this typically involves matrix-matrix multiplies with more dense intermediates.

IV. RESULTS

We have implemented these methods in the MondoSCF suite of linear scaling quantum chemistry programs.[51] The construction of the Fockian and derivative Fockian was carried out using the linear scaling QCTC method for computation of the Coulomb matrix[38,52] and the ONX algorithm[39,53] for computation of the Hartree–Fock exchange matrix. The CPSCF equations were solved, at each order, in an entirely orthogonal representation. Properties were evaluated using both the $n+1$ rule, given by Eq. (21), and the $2n+1$ rule, given by the nonorthogonal formulas in Eqs. (30) and (31). Two different levels of numerical accuracy have been used, `GOOD` and `TIGHT`. Thresholds that define the `GOOD` accuracy level include a matrix threshold $\tau=10^{-5}$, as well as other numerical thresholds detailed in Ref. 52, which deliver six digits of relative accuracy in the total energy. The `TIGHT` option involves the matrix threshold $\tau=10^{-6}$ and delivers eight digits of relative accuracy in the total energy.

Calculations were carried out on a single Intel Xeon 2.4-GHz processor running REDHAT LINUX 8.0 and executables compiled with Portland Group FORTRAN compiler PGF90 4.0-2.[54]

Convergence of the CPSCF equations for the water systems described in the following is typically achieved in about 10 cycles, independent of cluster size, basis set, matrix threshold, or order of the response calculated.

All results are reported in a.u. Also, unless otherwise noted, all timings and values have been obtained by computing the nth-order response function and evaluation with the $n+1$ rule (expectation value), Eq. (21).

A. One-dimensional water chains

Perturbed projection has been used to compute the (hyper)polarizabilities α_{zz}, β_{zzz}, and γ_{zzzz} of linear water chains up to $(H_2O)_{20}$. These calculations have been carried out with MondoSCF at the RHF/6-31G level of theory using both the `GOOD` and `TIGHT` thresholding parameters, as well as with the conventional algorithms implemented in the GAMESS quantum chemistry package.[55] These static properties have been evaluated at the geometries given by Otto *et al.*,[56] and the GAMESS results are given to the number of digits provided by that program. The MondoSCF results have been obtained both as expectation values, given by Eq. (21), and using the nonorthogonal density-matrix $2n+1$ rules given in Eqs. (30) and (31).

As a benchmark, we have also carried out calculations for the linear chain $(H_2O)_{20}$ with the `VERYTIGHT` numerical thresholding parameters, which employ a 10^{-7} drop tolerance and aim to provide ten digits of precision in the total energy. These `VERYTIGHT` calculations yield $\alpha_{zz}=7.142\,422$ a.u., $\beta_{zzz}=-12.033\,362$ a.u., and $\gamma_{zzzz}=1411.425\,500$ a.u.

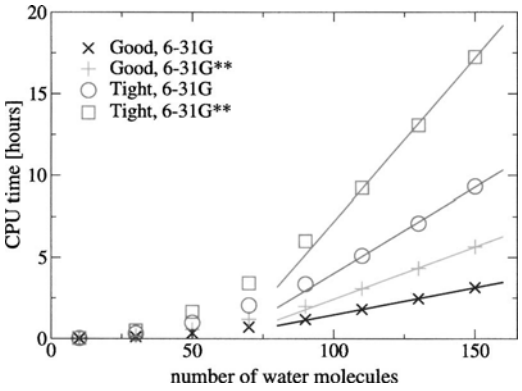

FIG. 1. Total CPU time of the fifth CPSCF iteration of fourth order for the water cluster sequence with the 6-31G and 6-31G** basis sets and the GOOD and TIGHT numerical thresholds (see text) controlling the numerical precision of the result. The lines are fits to the last three and four points, respectively.

B. Linear scaling: 3D water clusters

Linear scaling computation of the RHF/6-31G and RHF/6-31G** second hyperpolarizabilities, achieved with perturbed projection, is shown for three-dimensional water clusters in Fig. 1. These timings are the total CPU time for the fifth CPSCF cycle, including build time for $\mathcal{F}^{abc}$ (ONX and QCTC), iterative construction of $\mathcal{D}^{abc}$ (perturbed projection via TC2), and all intermediate steps including the congruence transformation. A breakdown of the dominant contributions to these totals is given in Figs. 2–4, which shows timings for Coulomb summation (QCTC), perturbed projection (TC2), and exact exchange (ONX).

Figure 5 shows the increase in cost associated with computing higher-order response functions. Corresponding to this increase in cost, Fig. 6 shows the magnitude of atom-atom blocks of density-matrix derivatives up to third order as a function of atom-atom distance when perturbed by a static electric field. The density response shows an approximate exponential decay as a function of internuclear distance with the rate of decay slowing slightly and the distribution shifted up with increasing order in the perturbation.

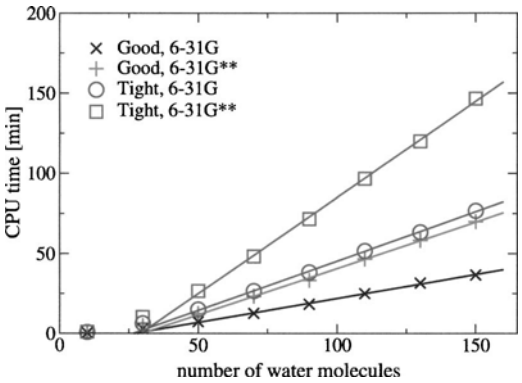

FIG. 2. QCTC CPU time of the fifth CPSCF iteration of fourth order for the water cluster sequence with the 6-31G and 6-31G** basis sets and the GOOD and TIGHT numerical thresholds (see text) controlling the numerical precision of the result. The lines are fits to the last three and four points, respectively.

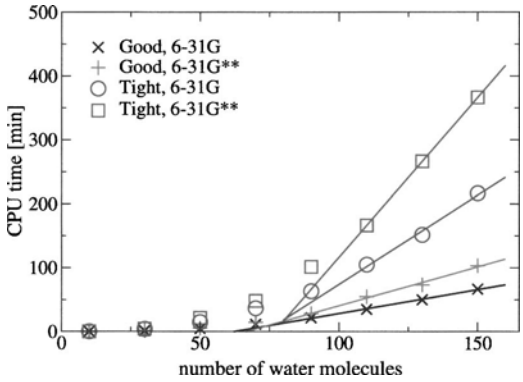

FIG. 3. TC2 CPU time of the fifth CPSCF iteration of fourth order for the water cluster sequence with the 6-31G and 6-31G** basis sets and the GOOD and TIGHT numerical thresholds (see text) controlling the numerical precision of the result. The lines are fits to the last three and four points, respectively.

V. DISCUSSION

In our current formulation, the increase in magnitude and reduction of locality in elements of the response function make achieving linear scaling more difficult with increasing order in perturbation. Nevertheless, linear scaling has been achieved at the HF level of theory up to fourth order (i.e., γ) in the total energy for three-dimensional systems and nontrivial basis sets. At fourth order, perturbed projection and exact exchange were the dominant costs in solving the CPSCF equations, as shown in Figs. 3 and 4. For the fourth-order perturbed projection, N scaling is achieved between 70 and 110 water molecules, depending on τ. Despite a nearly dense D^{abc}, the dominant work in its construction always involves multiplication with matrices that are significantly more sparse, as $\mathcal{X}_i^{abc}\mathcal{X}_i^0$ or $\mathcal{X}_i^{ab}\mathcal{X}_i^c$. Likewise, N scaling is achieved between 70 and 90 water molecules for construction of the Hartree–Fock exchange contribution. In this case, the approximate decay of the density matrix still leads to linear scaling through ordered skip out lists, as described in Ref. 39. In both cases, the increase in response function magnitude increases the cost and delays the onset of linear scaling. Likewise, the onset of linear scaling for more delocalized systems such as polyacetylene can be expected to occur

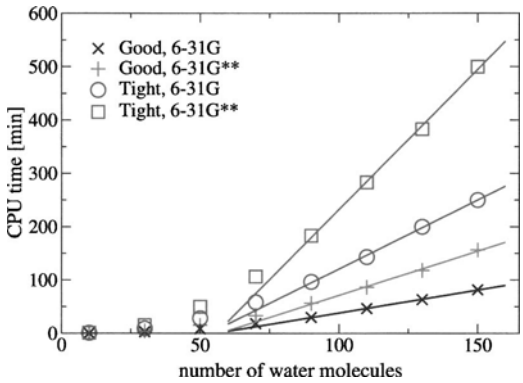

FIG. 4. ONX CPU time of the fifth CPSCF iteration of fourth order for the water cluster sequence with the 6-31G and 6-31G** basis sets and the GOOD and TIGHT numerical thresholds (see text) controlling the numerical precision of the result. The lines are fits to the last three and four points, respectively.

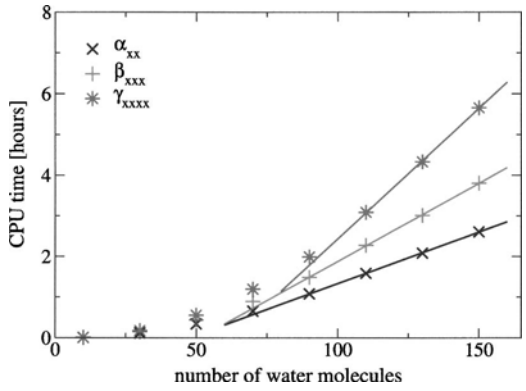

FIG. 5. Total CPU times with increasing order of the response for the fifth CPSCF cycle computed as the $n+1$ expectation value, Eq. (21).

later than for well-localized systems such as the water chains. This behavior is a desirable result of numerical thresholding; as the system becomes more delocalized, due to a narrowing gap or an increase in response order, the approximate matrices fill in to maintain a fixed accuracy.[23]

In Tables I–III we find that a reduction of the drop tolerance by one order of magnitude leads to an increase in precision by one to two significant digits, with GOOD and TIGHT yielding approximatively three to four and five to six correct digits independent of the response order. We further observe about one extra digit of accuracy when using the $2n+1$ rule. This might be expected from the higher-order error propagation resulting from products of lower-order response functions, relative to evaluation with Eq. (21), which involves an error that is always linear in a higher-order derivative density matrix.

As shown in Fig. 5, computing the second-order response is significantly cheaper than the third-order response, and involves an earlier onset of linear scaling. Because evaluation of properties with the $2n+1$ rule is of negligible cost relative to solving the CPSCF equations, the cost difference for evaluating γ with the $2n+1$ rule relative to the $n+1$ expectation is just the difference (roughly 2:3) between the computation of β and γ shown in Fig. 5.

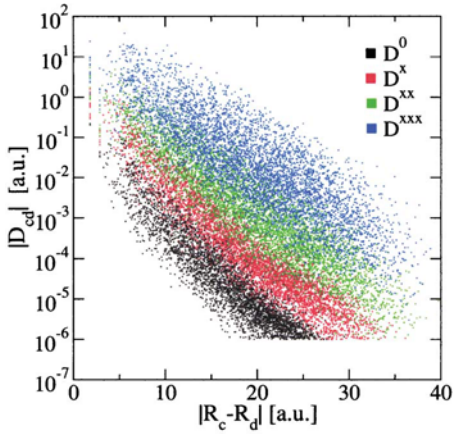

FIG. 6. (Color) Superposition of the magnitudes of the RHF/6-31G density-matrix derivative elements D_{cd}, D^{x}_{cd}, D^{xx}_{cd}, and D^{xxx}_{cd} along the x axis with the separation of basis function centers for $(H_2O)_{150}$. The density-matrix derivatives have been converged to within TIGHT (e.g., a matrix threshold $\tau = 10^{-6}$ a.u.).

TABLE I. The longitudinal polarizability, α_{zz}, for water chains at the RHF/6-31G level of theory, computed with MondoSCF using GOOD and TIGHT numerical thresholds, and also with the GAMESS quantum chemistry package (see Ref. 55).

N_{H_2O}	GAMESS	GOOD	TIGHT
1	5.8136	5.813 620	5.813 588
2	6.3448	6.345 037	6.344 822
3	6.5844	6.584 658	6.584 435
4	6.7276	6.727 905	6.727 672
5	6.8226	6.823 290	6.822 857
10	7.0308	7.031 056	7.030 858
15	7.1047	7.104 904	7.104 770
20	7.1424	7.142 580	7.142 422

VI. CONCLUSIONS

Linear scaling has been demonstrated for the computation of response properties beyond second order in the total energy using perturbed projection for solution of the coupled-perturbed self-consistent-field equations. In addition, we have provided details of the computational method, used three-dimensional systems and nontrivial basis sets to demonstrate linear scaling, and provided a (preliminary) assessment of error control. Perturbed projection for the computation of higher-order response functions is quadratically convergent, simple to implement through higher order, and numerically stable. Perturbed projection is not unique to the Hartree–Fock model, the TC2 generator, or the MondoSCF N-scaling algorithms, but can be straightforwardly extended to models that include exchange correlation (DFT), other purification schemes such as TRS4,[23] as well as to other electronic structure programs.

We have shown that response functions (density-matrix derivatives) through fourth order are local upon *global* electric perturbation, corresponding to an approximate exponential decay of matrix elements. However, the magnitude of the corresponding response function increases with increasing perturbation order, equivalent to tightening the matrix drop tolerance, τ. While we have not attempted to work out a detailed analysis for the propagation of error, it may be possible to develop a more effective thresholding scheme for higher orders. In addition to being somewhat more accurate, the $2n+1$ rule also provides a significantly

TABLE II. The longitudinal first hyperpolarizability, β_{zzz}, for water chains at the RHF/6-31G level of theory, computed with MondoSCF using GOOD and TIGHT numerical thresholds, and also with the GAMESS quantum chemistry package (see Ref. 55).

N_{H_2O}	GAMESS	GOOD	GOOD[a]	TIGHT	TIGHT[a]
1	−30.6125	−30.611 029	−30.612 627	−30.612 163	−30.612 256
2	−29.5444	−29.547 427	−29.548 604	−29.544 907	−29.544 994
3	−25.3696	−25.372 208	−25.373 615	−25.370 297	−25.370 381
4	−22.1411	−22.143 436	−22.145 040	−22.141 494	−22.141 603
5	−19.8925	−19.902 088	−19.904 449	−19.896 462	−19.897 141
10	−14.8063	−14.807 075	−29.617 990	−14.806 973	−14.807 119
15	−12.9713	−12.969 238	−12.972 227	−12.971 940	−12.972 124
20	−12.0334	−12.028 709	−12.033 633	−12.034 014	−12.034 238

[a]The density-matrix-based $2n+1$ rule has been used.

TABLE III. The longitudinal second hyperpolarizability, γ_{zzzz}, for water chains at the RHF/6-31G level of theory, computed with MondoSCF using GOOD and TIGHT numerical thresholds, and also with the GAMESS quantum chemistry package (see Ref. 55).

N_{H_2O}	GAMESS	GOOD	GOOD[a]	TIGHT	TIGHT[a]
1	330.5753	330.543 75	330.543 19	330.571 93	330.5724
2	820.1398	820.192 31	820.196 67	820.147 75	820.1493
3	1008.5656	1008.58 55	1008.60 73	1008.57 52	1008.5765
4	1103.4813	1103.50 53	1103.52 80	1103.48 83	1103.4902
5	1168.9563	1169.21 04	1169.25 31	1169.06 30	1169.0754
10	1324.2906	1325.12 08	1324.63 21	1324.29 75	1324.2999
15	1381.8657	1383.08 02	1382.23 22	1381.87 58	1381.8738
20	1411.4264	1414.40 92	1411.85 28	1411.44 10	1411.4292

[a]The density-matrix-based $2n+1$ rule has been used.

cheaper alternative to the computation of expectation values and an earlier onset of linear scaling.

A similar exponential decay in the first-order response corresponding to a *local* nuclear displacement has likewise been demonstrated by Ochsenfeld and Head-Gordon.[16] This behavior is expected to hold generally for both local and global perturbations to insulating systems. Thus, the potential exists for perturbed projection to achieve linear scaling for a large class of static molecular properties within the HF, DFT, and hybrid HF/DFT model chemistries. Of particular interest, the recently developed nonorthogonal density-matrix perturbation theory put forward in a proceeding article[30] may enable linear scaling computation of analytic second derivatives, which are important in computation of the Hessian matrix.

ACKNOWLEDGMENTS

This work has been supported by the US Department of Energy under Contract No. W-7405-ENG-36 and the ASCI project. The Advanced Computing Laboratory of Los Alamos National Laboratory is acknowledged. All the numerical computations have been performed on computing resources located at this facility.

[1] G. Galli, Curr. Opin. Solid State Mater. Sci. **1**, 864 (1996).
[2] D. R. Bowler, M. Aoki, C. M. Goringe, A. P. Horsfield, and D. G. Pettifor, Modell. Simul. Mater. Sci. Eng. **5**, 199 (1997).
[3] S. Goedecker, Rev. Mod. Phys. **71**, 1085 (1999).
[4] P. Ordejon, Phys. Status Solidi B **217**, 335 (2000).
[5] V. Gogonea, D. Suarez, A. van der Vaart, and K. W. Merz, Curr. Opin. Struct. Biol. **11**, 217 (2001).
[6] S. Y. Wu and C. S. Jayanthi, Phys. Rep. **358**, 1 (2002).
[7] H. Sekino and R. J. Bartlett, J. Chem. Phys. **85**, 976 (1986).
[8] S. P. Karna and M. Dupuis, J. Comput. Chem. **12**, 487 (1991).
[9] K. Wolinski, J. F. Hinton, and P. Pulay, J. Am. Chem. Soc. **112**, 8251 (1990).
[10] C. H. Pennington and C. P. Slichter, Phys. Rev. Lett. **66**, 381 (1991).
[11] O. L. Malkina, D. R. Salahub, and V. G. Malkin, J. Chem. Phys. **105**, 8793 (1996).
[12] R. Amos and J. E. Rice, Comput. Phys. Rep. **10**, 147 (1989).
[13] M. Lazzeri and F. Mauri, Phys. Rev. Lett. **90**, 036401 (2003).
[14] O. Quinet and B. Champagne, J. Chem. Phys. **115**, 6293 (2001).
[15] J. Pople, R. Krishnan, H. B. Schlegel, and J. S. Binkley, Int. J. Quantum Chem. **S13**, 225 (1979).
[16] C. Ochsenfeld and M. Head-Gordon, Chem. Phys. Lett. **270**, 399 (1997).
[17] H. Larsen, T. Helgaker, J. Olsen, and P. Jorgensen, J. Chem. Phys. **115**, 10344 (2001).
[18] C. Ochsenfeld, J. Kussmann, and F. Koziol, Angew. Chem. **43**, 4485 (2004).
[19] J. Brandts, Lect. Notes Comput. Sci. **2179**, 462 (2001).
[20] V. Weber, A. M. N. Niklasson, and M. Challacombe, Phys. Rev. Lett. **92**, 193002 (2004).
[21] A. M. N. Niklasson and M. Challacombe, Phys. Rev. Lett. **92**, 193001 (2004).
[22] A. M. N. Niklasson, Phys. Rev. B **66**, 155115 (2002).
[23] A. M. N. Niklasson, C. J. Tymczak, and M. Challacombe, J. Chem. Phys. **118**, 8611 (2003).
[24] R. McWeeny, Rev. Mod. Phys. **32**, 335 (1960).
[25] W. L. Clinton, A. J. Galli, and L. J. Massa, Phys. Rev. **177** 7 (1969).
[26] A. H. R. Palser and D. E. Manolopoulos, Phys. Rev. B **58**, 12704 (1998).
[27] G. Beylkin, N. Coult, and M. J. Mohlenkamp, J. Comput. Phys. **152**, 32 (1999).
[28] K. Nemeth and G. E. Scuseria, J. Chem. Phys. **113**, 6035 (2000).
[29] A. Holas, Chem. Phys. Lett. **340**, 552 (2001).
[30] A. M. N. Niklasson, V. Weber, and M. Challacombe, J. Chem. Phys. **123** 044107 (2005).
[31] A. M. Lee and S. M. Colwell, J. Chem. Phys. **101**, 9704 (1994).
[32] P. Salek, O. Vahtras, T. Helgaker, and H. Ågren, J. Chem. Phys. **117**, 9630 (2002).
[33] J. H. Wilkinson, *The Algebraic Eigenvalue Problem* (Clarendon, Oxford, 1965).
[34] G. W. Stewart, *Introduction to Matrix Computations* (Academic, London, 1973).
[35] M. Benzi and C. D. Meyer, SIAM J. Sci. Comput. (USA) **16**, 1159 (1995).
[36] M. Benzi, C. D. Meyer, and M. Tůma, SIAM J. Sci. Comput. (USA) **17**, 1135 (1996).
[37] M. Benzi, R. K. R, and M. Tuma, Comput. Methods Appl. Mech. Eng. **190**, 6533 (2001).
[38] M. Challacombe and E. Schwegler, J. Chem. Phys. **106**, 5526 (1997).
[39] E. Schwegler, M. Challacombe, and M. Head-Gordon, J. Chem. Phys. **106**, 9708 (1997).
[40] F. Furche, J. Chem. Phys. **114**, 5982 (2001).
[41] M. Challacombe, Comput. Phys. Commun. **128**, 93 (2000).
[42] V. Weber and C. Daul, Chem. Phys. Lett. **370**, 99 (2003).
[43] S. Goedecker, J. Comput. Phys. **118**, 261 (1995).
[44] W. Z. Liang, C. Saravanan, Y. Shao, R. Baer, A. T. Bell, and M. Head-Gordon, J. Chem. Phys. **119**, 4117 (2003).
[45] W. Liang, R. Baer, C. Saravanan, Y. H. Shao, A. Bell, and M. Head-Gordon, J. Comput. Phys. **194**, 575 (2004).
[46] A. F. Voter, J. D. Kress, and R. N. Silver, Phys. Rev. B **53**, 12733 (1996).
[47] P. Pulay, Chem. Phys. Lett. **73**, 393 (1980).
[48] P. Pulay, J. Comput. Chem. **3**, 556 (1982).
[49] S. T. Epstein, *The Variation Method in Quantum Chemistry* (Academic, San Fransisco, 1974).
[50] R. McWeeny, Phys. Rev. **126**, 1028 (1962).
[51] M. Challacombe, E. Schwegler, C. J. Tymczak, C. K. Gan, K. Nemeth, V. Weber, A. M. N. Niklasson, and G. Henkelman, MondoSCF *v1.0α9*, a program suite for massively parallel, linear scaling SCF theory and *ab initio* molecular dynamics, (2001); http://www.t12.lanl.gov/home/mchalla/, Los Alamos National Laboratory (LA-CC 01-2), Copyright University of California.
[52] C. J. Tymczak and M. Challacombe, J. Chem. Phys. **122** 134102 (2005).
[53] C. J. Tymczak, V. Weber, E. Schwegler, and M. Challacombe, J. Chem. Phys. **122** 124105 (2005).
[54] The Portland Group, *PGF90 v4.2* (2002); http://www.pgroup.com/
[55] M. W. Schmidt, K. K. Baldridge, J. A. Boatz, *et al.* J. Comput. Chem. **14**, 1347 (1993).
[56] P. Otto, F. L. Gu, and J. Ladik, J. Chem. Phys. **110**, 2717 (1999).